

THE EFFECT OF ADDITION OF TWO TARGETED VECTORS, cRGD PEPTIDE AND FOLIC ACID, WITH THE SAME LINKER LENGTH ON THE PROPERTIES OF THE DOXORUBICIN PHOSPHOLIPID COMPOSITION: A STUDY OF PROPERTIES *IN VITRO*

L.V. Kostryukova*, Yu.A. Tereshkina, F.N. Bedretdinov, A.M. Gisina

Institute of Biomedical Chemistry,
10 Pogodinskaya str., Moscow, 119121 Russia; *e-mail: kostryukova87@gmail.com

Serious side effects of the chemotherapeutic drug doxorubicin prompt researchers to develop systems for its targeted delivery to cells. In this work, we continued the study on the effect of using two vectors in a phospholipid delivery system of doxorubicin (Dox) for targeted therapy of breast cancer. We have obtained a composition NPh-Dox-cRGD-Fol(2.0) with the same linker length for both targeting ligands, cRGD and folic acid (PEG 2000). The resulting composition NPh-Dox-cRGD-Fol(2.0) with a particle size less than 50 nm and with 99% Dox incorporated into nanoparticles in an experiment on drug release at different pH values (5.0 and 7.4) showed a faster release and a high level of Dox compared to the phospholipid nanoform and a composition containing only the cRGD peptide. *In vitro* experiments on MDA-MB-231 breast cancer cells expressing the folate receptor and integrin $\alpha_v\beta_3$ demonstrated an increase in the total accumulation and internalization of Dox upon incubation with the dual-vector composition compared to the control samples. On the MCF-7 breast cancer cell line (expressing only the folate receptor), a similar effect was observed upon incubation with the single-vector composition containing folic acid (NPh-Dox-Fol(2.0)). In experiments with normal Wi-38 cell line, the internalization and total accumulation of the drug were comparable for both the free substance and the vector compositions. After 24 h incubation of MDA-MB-231 cells with Dox-containing (10 $\mu\text{g/ml}$ Dox) samples, the lowest percentage of living cells was observed for the studied dual-vector composition NPh-Dox-cRGD-Fol(2.0). On MCF-7 cells, the cytotoxic effect was manifested equally for the studied samples. The study of the cell death pathway on MDA-MB-231 cells showed the predominance of the apoptotic pathway (late apoptosis), while in the case of MCF-7 the necrosis pathway predominated. The cell cycle study performed using MDA-MB-231 cells (folate receptor (+) and integrin $\alpha_v\beta_3$ (+)) revealed an increase in the percentage of cells in the G0/G1 phase was noted thus indicating apoptotic cell death during incubation with NPh-Dox-cRGD-Fol(2.0). No differences were found between the samples in experiments performed on MCF-7 cells (folate receptor (+) and integrin $\alpha_v\beta_3$ (-)).

Keywords: doxorubicin; phospholipid nanoparticles; breast cancer; cRGD peptide; folic acid; FR α

DOI: 10.18097/PBMCR1538

INTRODUCTION

Oncological diseases are one of the major public health problems. The most common types of cancers are: breast cancer, skin cancer, prostate cancer, uterine cancer, and colon cancer [1]. The priority classical method of treating malignant neoplasms is chemotherapy. Doxorubicin (Dox) is the most widely used drug for chemotherapy of various types of cancer, including breast cancer [2]. The cytotoxic effect of Dox is characterized by several mechanisms, such as: (1) DNA intercalation and adduct formation; (2) inhibition of topoisomerase II (TopII); (3) generation of free radicals, oxidative stress; (4) membrane damage due to changes in sphingolipid metabolism [3]. However, despite the high efficacy of Dox, its use is limited by serious side effects (such as cardiotoxicity, multidrug resistance, etc.) [4–8]. The use of nanotechnology and the development of nanoparticles (NPs) can reduce the systemic side effects of chemotherapeutic agents and increase their therapeutic efficacy. Delivery of drugs in NPs to tumor cells is mediated

by the pathophysiological properties of the tumor, in particular its increased permeability, retention effect, and its microenvironment [9]. Promising ligands for drug delivery to the tumor are peptides containing the Asn-Gly-Arg (RGD) sequence. They exhibit affinity for cell surface integrins ($\alpha_v\beta_3$ and $\alpha_5\beta_1$), which are involved in cell attachment to the extracellular matrix [10]. Integrin $\alpha_v\beta_3$ is involved in the processes of proliferation, invasion, and metastasis of tumor cells, in particular breast cancer. Integrin-mediated cell adhesion includes activation of a number of kinases [11, 12]. Cyclization of RGD peptides increases their stability by reducing conformational flexibility and susceptibility to proteolysis [13, 14].

Folic acid, interacting with the folate receptor (FR), is also a promising targeted agent in the delivery of drugs to the tumor. FR is a protein associated with glycosylphosphatidylinositol. It is basically not expressed in normal cells, while its increased expression is observed on some tumor cells [15]. Folic acid binds to FR, which promotes its penetration



into the cell via endocytosis, with subsequent release in endosomes [16, 17]. Thus, folic acid can be used as an active targeting agent in delivery systems to increase the efficiency of the transported drug.

Many authors proposed a promising approach based on combined use of several targeted ligands in one delivery system for antitumor drugs [18]. In this work, based on studies in this area [18], as well as previously obtained positive results on the incorporation of Dox into phospholipid NPs with two targeted conjugates (DSPE-PEG2000-cRGD and DSPE-PEG3400-Folat) [19], we obtained a two-vector Dox composition containing a cRGD peptide and folic acid with the same linker length (PEG2000). The aim of the work was to study the physical properties of the obtained composition and its interaction with breast cancer cells *in vitro*, including cellular accumulation of Dox, cytotoxicity, as well as cell death pathways and the cell cycle.

MATERIALS AND METHODS

Materials

The substance of doxorubicin hydrochloride (purity 99%) was obtained from the Omutninsk Scientific Experimental and Production Base (Russia). NPs were prepared using soy phosphatidylcholine Lipoid S100 (Lipoid, Germany). The targeted cyclic peptide cRGDfC with purity of at least 95%, confirmed by HPLC with mass spectrometric detection and NMR spectroscopy, was obtained from Sinton-Lab (Russia). DSPE-PEG2000-Maleimide (Nanosoft Polymers, USA) was used to incorporate the targeted peptide into phospholipid NPs. The DSPE-PEG2000-Folate conjugate (Nanosoft Polymers) was used as the second targeted fragment. Phosphate buffered saline (PBS) (PanEco, Russia) and 96% ethanol (Medkhimprom, Russia) were also used in the study. Distilled water was prepared using a GFL-2004 distiller (GFL, Germany).

Cell cultures were incubated using DMEM medium, Versen solution (PanEco), and fetal bovine serum (FBS) (Gibco, USA).

Tumor cell viability was assessed using the MTT assay (Mumbai, India). Cell death pathways were assessed using a commercial kit for determining apoptotic cells by means of annexin V-AF488 and propidium iodide (Lumiprobe, Russia), consisting of annexin V conjugated with AF488, propidium iodide (PI) and annexin binding buffer. Cell cycle assessment was performed using RNAs (Thermo Scientific, Latvia).

Cell Lines

Human breast cancer cell lines (MDA-MB-231 and MCF-7) and a human diploid cell line (Wi-38) obtained from the American Collection and maintained

in the Cell Culture Collection (Institute of Biomedical Chemistry; IBMC) were used in the work. Cell lines were identified using the autosomal STR loci analysis technology (Gordiz, Russia). Tumor cells were cultured in accordance with the recommendations specified in the cell culture certificates. Cells were incubated in DMEM culture medium containing 2 mM L-glutamine and 10% FBS in 25 cm² and 75 cm² culture flasks (Biologix, China) at 37°C in a humidified atmosphere with 5% CO₂ in a Sanyo CO₂ incubator (Sanyo, Japan).

Preparation of Dox Phospholipid Compositions

A DSPE-PEG2000-cRGD conjugate was prepared according to a previously described method [34, 35]. Dox compositions with targeting agents, folic acid and cRGD peptide (NPh-Dox-cRGD, NPh-Dox-Fol(2.0), and NPh-Dox-cRGD-Fol(2.0)), were prepared as described previously [28]. Phospholipid compositions were prepared by the film method using soy phospholipid Lipoid S100 and targeting conjugates. The Dox : Lipoid and Lipoid : conjugate (cRGD or Folate) ratios were 1:20 (w/w). The obtained Dox-containing compositions were analyzed for particle size, zeta (ζ) potential using Zetasizer Malvern ZS (Malvern Instruments Ltd., UK), drug concentration and percentage of its inclusion in NPs using an Agilent 1100 series liquid chromatograph (Agilent Technologies, USA) with diode array detector and ChemStation Rev. A.09.03 software.

In Vitro Dox Release from NPs

Dox release from NPs (with and without targeted conjugate) was assessed using dialysis bags (cutoff threshold 3.5 kDa) (Spectrum Labs, Greece). Briefly, 1 ml of test samples (1 mg/ml Dox) in dialysis bags were placed in 25 ml of PBS (pH 7.4 and 5.0), then incubated and mixed at 37°C and 100 rpm in a Grant OLS 200 shaker water bath (Grant Instruments (Cambridge) Ltd., UK). Aliquots of the supernatant (1 ml) were collected at certain time intervals for each sample (0.25 h, 0.5 h, 1 h, 2 h, 3 h, 5 h, 24 h, 48 h, and 72 h). An equal volume of PBS was added after each sampling. The concentration was determined using an Agilent 8453 spectrophotometer (Agilent Technologies) at 254 nm. The drug release rate was calculated by dividing the drug concentration (the drug released from the phospholipid NPs) at a given time by the initial drug concentration in the phospholipid NPs [20].

Evaluation of Cell Binding and Penetrating Ability

Cells of MDA-MB-231, MCF-7, and Wi-38 (10⁶ cells per well) were seeded in 6-well culture plates (Biologix) and incubated for 24 h at 37°C. Free Dox substance was used as a reference (control). Samples of the obtained compositions and free substance (10 µg/ml in terms of Dox) were incubated

for 24 h at two temperatures: at 37°C in a CO₂ incubator (Sanyo) and 4°C in a refrigerator (ATLANT, Belarus). After incubation and removal of the medium, the cells were washed twice with PBS. Dox was extracted with acetonitrile solution (CARLO ERBA Reagents GmbH, Italy) with the addition of 0.1% formic acid (Acros Organics, USA) (1 ml per well). The collected extracts were separated by centrifugation at 10,000 rpm for 10 min in a MiniSpin plus benchtop centrifuge (Eppendorf, rotor F-45-12-11, Germany). The Dox concentration in the obtained samples was measured using an Agilent 1200 Series HPLC system equipped with an Eclipse XDB-C18 column (Agilent Technologies) and a 6130 Quadrupole LC/MS mass spectrometric detector (Agilent Technologies). The Dox content in cell cultures was normalized to the protein content (mg), which was determined by the Lowry colorimetric method.

Internalization was calculated as the difference in the Dox content at 37°C (total accumulation in cells) and at 4°C (binding to the cell surface [21]).

In Vitro Cytotoxicity Analysis

The cytotoxicity of the developed Dox formulations was assessed *in vitro* using the MTT test. MDA-MB-231, MCF-7, and Wi-38 cells (10⁵ cells/well) were seeded in sterile 96-well culture plates and incubated in a CO₂ incubator at 37°C in 5% CO₂ for 24–26 h. Then, the studied samples were added at Dox concentrations of 0.125 µg/ml, 0.25 µg/ml, 0.5 µg/ml, 1 µg/ml, 2.5 µg/ml, 5 µg/ml, and 10 µg/ml and the cells were incubated for 24 h and 48 h. After that, 50 µl of MTT (1 mg/ml) was carefully added to each well and incubated at 37°C for 3 h. Then, the medium was carefully removed and 100 µl DMSO (PanEco) was added. The plates were covered with foil and shaken on an orbital shaker for 15 min. Absorbance was recorded at 570 nm using a Multiscan FC (ThermoSpectronic, USA) and normalized to the Dox-free control.

In Vitro Cell Death Pathway Analysis

The cells were cultured in 6-well plates until a monolayer of 80–90% was achieved. Then, the studied samples (Dox, NPh-Dox, NPh-Dox-cRGD, NPh-Dox-Fol(2.0), and NPh-Dox-cRGD-Fol(2.0)) were added to the medium (Dox concentration 0.5 µg/ml) and incubated for 24 h (37°C, 5% CO₂). Then, the cells were washed from the medium twice with Hanks' solution, and after addition of trypsin and Versene solutions (1:1) the resulting mixture was suspended by pipetting. Then, the cells were washed once in PBS by centrifugation at 1000 rpm using a MiniSpin plus (Eppendorf, rotor F-45-12-11) for 4 min. The resulting pellet was resuspended in 100 µl of binding buffer. The cells were incubated with 5 µl of annexin V-AF488 in the dark for 15 min at room temperature. After subsequent addition (without

preliminary washing) of 400 µl of 1x annexin V binding buffer (included in the commercial kit) into to each tube, PI was added and the cells were incubated for 5 min in the dark at room temperature. Cell staining was analyzed using a FACSaria III flow cytometer sorter (BD Biosciences, USA) equipped with blue (488 nm) and yellow-green (561 nm) lasers. The results were analyzed using BD FACSDiva version 7 software. Data were graphically represented using FlowJo version 10.

In Vitro Cell Cycle Analysis

MDA-MB-231, MCF-7, and Wi-38 cells (10⁶ cells per well) were seeded in 6-well culture plates (Biologyx) and incubated for 24 h at 37°C. The studied Dox samples (Dox, NPh-Dox, NPh-Dox-cRGD, NPh-Dox-Fol(2.0), and NPh-Dox-cRGD-Fol(2.0)) were then added to the medium at a Dox concentration of 3 µg/ml and incubated for 24 h (37°C, 5% CO₂). The cells were washed twice with a trypsin-Versene solution (1:1). The cell suspension was then washed twice more with cold PBS and centrifuged at 1000 rpm for 4 min in a MiniSpin plus centrifuge. The cell pellet was fixed with cold 70% ethanol. After fixation, 2 µl of RNAs (10 mg/ml) (Thermo Scientific) were added to the cells and they were incubated for 30 min at 37°C. Then, 400 µl of PBS and 5 µl of PI were sequentially added to the cells. Cell staining was analyzed using a FACSaria III flow cytometer sorter (BD Biosciences) equipped with blue (488 nm) and yellow-green (561 nm) lasers. The results were analyzed using BD FACSDiva version 7 software. Graphical representation of the data was obtained using FlowJo version 10.

Statistical Processing

Student's *t*-test was used to assess the significance of differences in the measured parameters for three replicates. Differences were considered statistically significant at $p \leq 0.05$. The data in the figures are presented as mean \pm standard deviation.

RESULTS AND DISCUSSION

The use of Dox for the treatment of malignant neoplasms is limited by its side effects due to non-specific distribution in the body [5, 7]. Many studies are aimed at overcoming these drawbacks by incorporating the drug into delivery systems [22]. To reduce nonspecific distribution and increase drug accumulation in tumor cells, several targeting fragments can be used in drug delivery systems [18]. The simultaneous use of targeting peptides with the RGD motif, binding to the integrin $\alpha_v\beta_3$ involved in tumor adhesion and metastasis, and folic acid, binding to FR, which is highly expressed on the surface of breast cancer cells [23], was previously shown by us in a phospholipid system for Dox delivery [19]. It should be noted that different linker lengths were used for each vector

DOXORUBICIN COMPOSITION WITH THE SAME LENGTH OF LINKERS

component: PEG2000 (for the cRGD peptide) and PEG3400 (for folic acid) [19]. The particle size of the developed composition was 39.62 ± 4.61 nm, and the ζ -potential was 4.17 ± 0.83 mV, the total accumulation and internalization of Dox on MDA-MB-231 cells during incubation with this composition was ~ 1.4 and ~ 1.3 times higher compared to monovector compositions. In this regard, it was important to establish a relationship between the linker length used for the vectors and the properties of the resulting composition. Therefore, in this work, a composition of Dox embedded in phospholipid NPs with two addressable fragments having the same linker length (PEG2000) was obtained — NPh-Dox-cRGD-Fol(2.0) and its properties were studied. Compositions with each individual component, including phospholipid composition (NPh-Dox), phospholipid composition with cRGD peptide (NPh-Dox-cRGD), and phospholipid composition with folic acid (NPh-Dox-Fol(2.0)) were used as reference samples.

To assess the properties and stability of nanopreparations, including liposomal ones, 3 main parameters are used: the size of NPs, the polydispersity index (Pdl) and the ζ -potential. The results of the study of physicochemical properties of the studied compositions are presented in Table 1. The particle size in all samples was less than 50 nm. The addition of targeted conjugates led to an enlargement of the particles compared to the initial composition (NPh-Dox). In the sample with two vectors NPh-Dox-cRGD-Fol(2.0) the particle size was maximal (48.65 ± 2.93 nm). In the other samples the value of this parameter decreased in the following order: NPh-Dox-cRGD and NPh-Dox-Fol(2.0). Comparison of the obtained particle size values with the parameters of the previously developed composition [19], has shown that the use of a shorter linker length did not lead to a decrease in the particle size.

In phospholipid emulsions, NPs in one system can be non-uniform in size, i.e. polydisperse. For drug delivery systems based on lipid vesicles, a Pdl value of 0.3 and below is considered satisfactory, indicating a relatively homogeneous population of lipid vesicles [25]. In our study, Dox compositions with targeted fragments

had Pdl values below 0.3, indicating their relative homogeneity. Addition of address fragments increased the homogeneity of nanoemulsions. The Pdl value in the NPh-Dox composition was higher than the values for compositions with address components and was close to 0.3. Thus, according to the obtained results for the Pdl value, the insertion of address fragments (cRGD and Fol(2.0)) led to an increase in the homogeneity of the phospholipid composition.

The ζ -potential value characterizes the aggregation stability of particles in a nanoemulsion: the greater its absolute value, the greater the surface charge of the particles is. This ensures their electrostatic stabilization and increases the forces of electrostatic repulsion between the particles, protecting them from aggregation. According to the classification of NP dispersions by the ζ -potential value [26], the obtained NPh-Dox-cRGD-Fol(2.0) composition is unstable (ζ -potential values are within ± 0 –10 mV); the NPh-Dox composition is relatively stable (ζ -potential ± 10 –20 mV). For the remaining samples, the ζ -potential value was within 10 mV. Thus the incorporation of address components into the composition led to a decrease in the surface charge of the particles, especially when they were incorporated simultaneously (Table 1, Fig. 1B). In our previous study, we obtained similar values for a composition with different linker lengths for vector ligands, but all samples were sufficiently stable in various solutions (incubation medium, H₂O, PBS) for 3 days at 25°C [19]. Evaluation of Dox incorporation into NPs showed almost complete incorporation of the substance (100%) in all samples.

The study of the release of the active component (the drug substance) from NPs can predict the “behavior” of the obtained nanocomposition under certain biological conditions. In endosomes or lysosomes of tumor cells, the natural pH gradient is 4.0–6.5, while in the tumor microenvironment it is 6.5–7.2 [27]. Thus, modeling of these conditions will help to understand the degree and time of Dox release from phospholipid NPs.

Incubation of the studied samples of phospholipid compositions in PBS with pH 7.4 (Fig. 2A), was accompanied by a gradual increase in the drug level in the solution. In the case of NPh-Dox-Fol(2.0) and NPh-Dox-cRGD-Fol(2.0), the maximum release of Dox

Table 1. Characteristics of the obtained compositions by particle size and the polydispersity index

Compositions	Particle size, nm / % of particles of a given size	Polydispersity index (Pdl)	ζ -potential, mV	Percentage of Dox included in NP, %
NPh-Dox	19.63 ± 0.94 ($99.93 \pm 0.06\%$)	0.344 ± 0.049	13.50 ± 3.83	99.07 ± 0.65
NPh-Dox-cRGD	37.58 ± 1.23 ($99.67 \pm 0.40\%$)	0.258 ± 0.050	8.77 ± 1.46	99.44 ± 0.23
NPh-Dox-Fol(2,0)	36.50 ± 1.75 ($99.06 \pm 0.82\%$)	0.254 ± 0.015	5.72 ± 0.40	98.89 ± 0.81
NPh-Dox-cRGD-Fol(2,0)	48.65 ± 2.93 ($98.76 \pm 0.21\%$)	0.249 ± 0.056	3.29 ± 0.84	98.98 ± 0.88

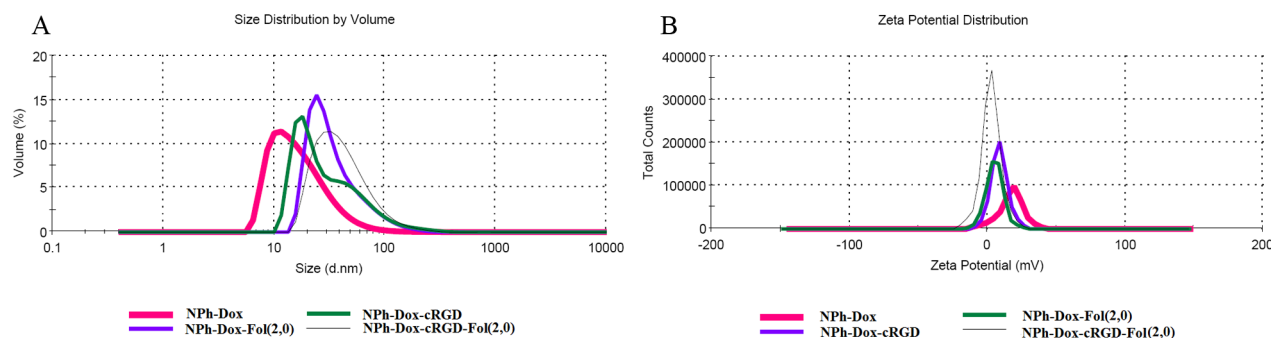


Figure 1. Particle size distribution (A) and ζ -potential of aqueous solutions (B) of phospholipid compositions containing Dox.

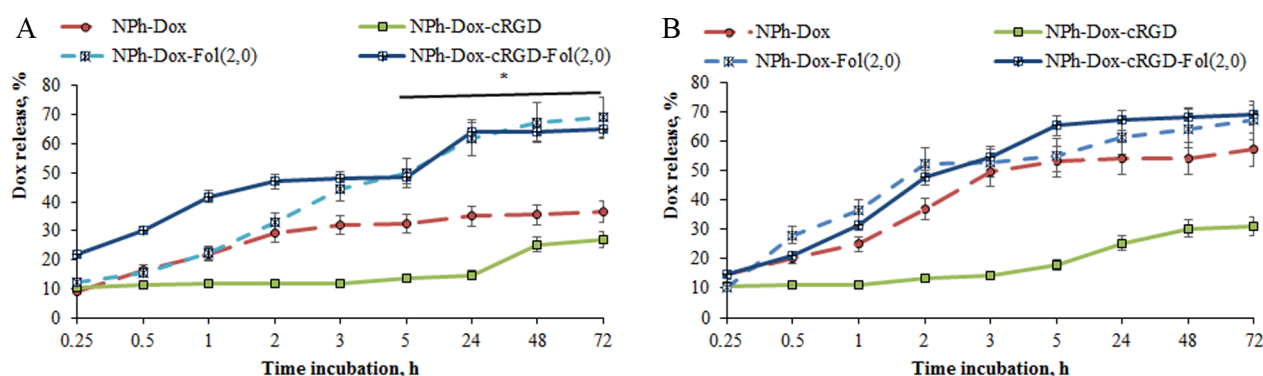


Figure 2. Dox release of from NPs by dialysis during incubation of the studied phospholipid compositions in solutions with pH 7.4 (A) and 5.0 (B). * $p < 0.05$ compared to the phospholipid nanoform (NPh-Dox).

was noted after 5 h (about 50% of the initial content). In the case of other phospholipid compositions, the level of Dox release was lower (within 40%). At pH 5.0 (Fig. 2B), a faster release of Dox from the NPs was observed. After 2 h incubation, the Dox release was about 42–50% in the case of NPh-Dox-Fol(2,0) and NPh-Dox-cRGD-Fol(2,0), while in the case of other samples phospholipid compositions, the release did not exceed 30%. After 72 h incubation, the Dox release reached 68% in the case of NPh-Dox-Fol(2,0) and NPh-Dox-cRGD-Fol(2,0).

Evaluation of Dox accumulation in cells during incubation with the studied phospholipid compositions *in vitro* was carried out on breast cancer cell lines MDA-MB-231 and MCF-7, and also human fibroblasts Wi-38 (used as control). In this study, the integrin $\alpha_v\beta_3$, responsible for adhesion and metastasis, and FR were considered as cell surface-expressed targets. According to the literature data, both integrin $\alpha_v\beta_3$ and FR are detected on the cell surface of MDA-MB-231 [28, 29], integrin $\alpha_v\beta_3$ is absent on the surface of MCF-7 cells [30], but FR is detected [31]. Human fibroblast cells Wi-38 do not express FR, but integrin $\alpha_v\beta_3$ is detected on their surface [32, 33].

The study of cellular drug accumulation was carried out after 24 h incubation of the selected cell lines with the developed compositions (Dox concentration 10 $\mu\text{g/ml}$). In the case

of MDA-MB-231 cells, the maximal total accumulation was noted for the variants of the compositions with two vectors (Fig. 3A). This value was more than 2 times higher than for the free substance and 35% higher than for the phospholipid composition. The presence of each vector separately in the composition increased the level of total drug accumulation; however, the effect of folic acid was higher than the effect of the cRGD peptide.

Attachment to the cell surface was the same for NPh-Dox, NPh-Dox-cRGD, and NPh-Dox-cRGD-Fol(2,0). At the same time, the amount of Dox bound to the cell surface was 30% higher than for the free substance and the composition with two peptides. However, the calculation of internalization showed a greater effect for NPh-Dox-cRGD-Fol(2,0) compared to both the composition with folic acid (NPh-Dox-Fol(2,0)), and especially with the free substance. The influence of RGD peptide on Dox internalization was minimal, with values comparable to those of the phospholipid form (NPh-Dox).

Certain differences have been found during evaluation of Dox accumulation in the case of the second breast cancer cell line MCF-7 (Fig. 3B), which expresses only the FR on its surface [31]. The maximal total accumulation of Dox (at 37°C) was noted for the NPh-Dox-Fol(2,0) composition; it was 2.4 and 3.11 times higher than in the case

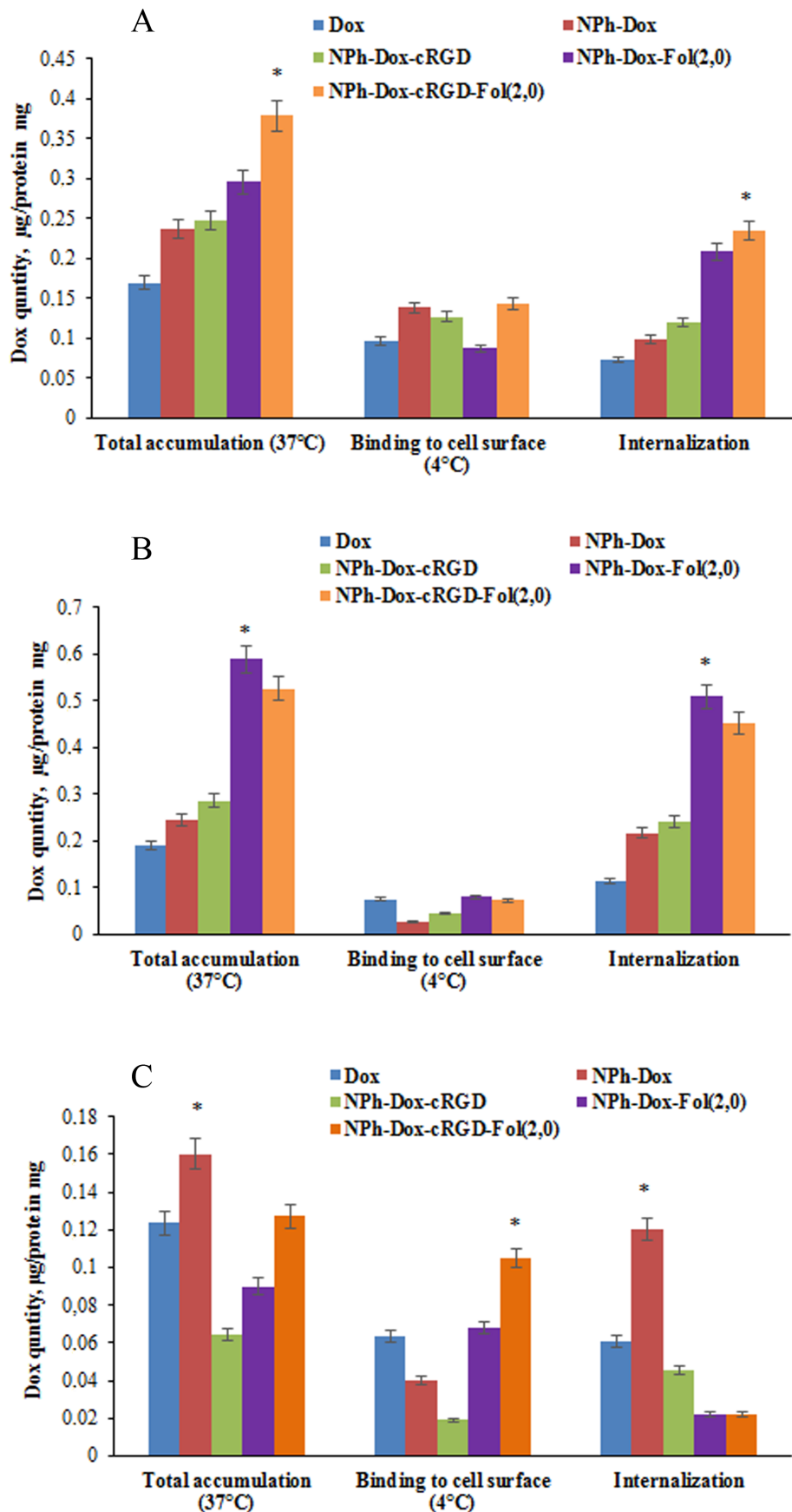


Figure 3. Dox accumulation of in MDA-MB-231 (A), MCF-7 (B), and Wi-38 (C) cells after 24 h of incubation with Dox compositions and free Dox (Dox concentration 10 $\mu\text{g/ml}$). Data are presented as mean \pm standard deviation (n=3). * $p < 0,05$ compared to free substance (Dox).

of the phospholipid nanoform and the free substance, respectively. For NPh-Dox-cRGD-Fol(2.0), the level of total Dox accumulation was more than 2 times higher than in the case of the phospholipid form. For the composition with the peptide (NPh-Dox-cRGD), the value of total Dox accumulation was expectedly close to the phospholipid form due to the absence of integrin $\alpha_v\beta_3$ on the surface of this cell line [53] (but the presence of FR). Dox binding to the cell surface was lower than for the previous cell line. Calculation of the amount of Dox that internalized into the cell showed the same effect as in the total accumulation, where the maximal amount of Dox was detected during incubation with NPh-Dox-Fol(2.0). At the same time, for NPh-Dox-cRGD-Fol(2.0), this value was slightly lower compared to the composition

containing only folic acid (by 11.3%). It can be assumed that in this case, the presence of the RGD peptide in the composition somehow interfered with the penetration of the drug into the cell.

For all compositions containing targeted components, the values of total accumulation and internalization on the Wi-38 cells (Fig. 3B) were lower compared to the phospholipid nanoform. Attachment to the cell surface was unexpectedly maximal for the composition containing two vectors (NPh-Dox-cRGD-Fol(2.0)).

The cytotoxic effect of the obtained compositions was studied using the MDA-MB-231, MCF-7, and Wi-38 cell lines. The results of the study showed a dose-dependent effect for all compositions (Fig. 4).

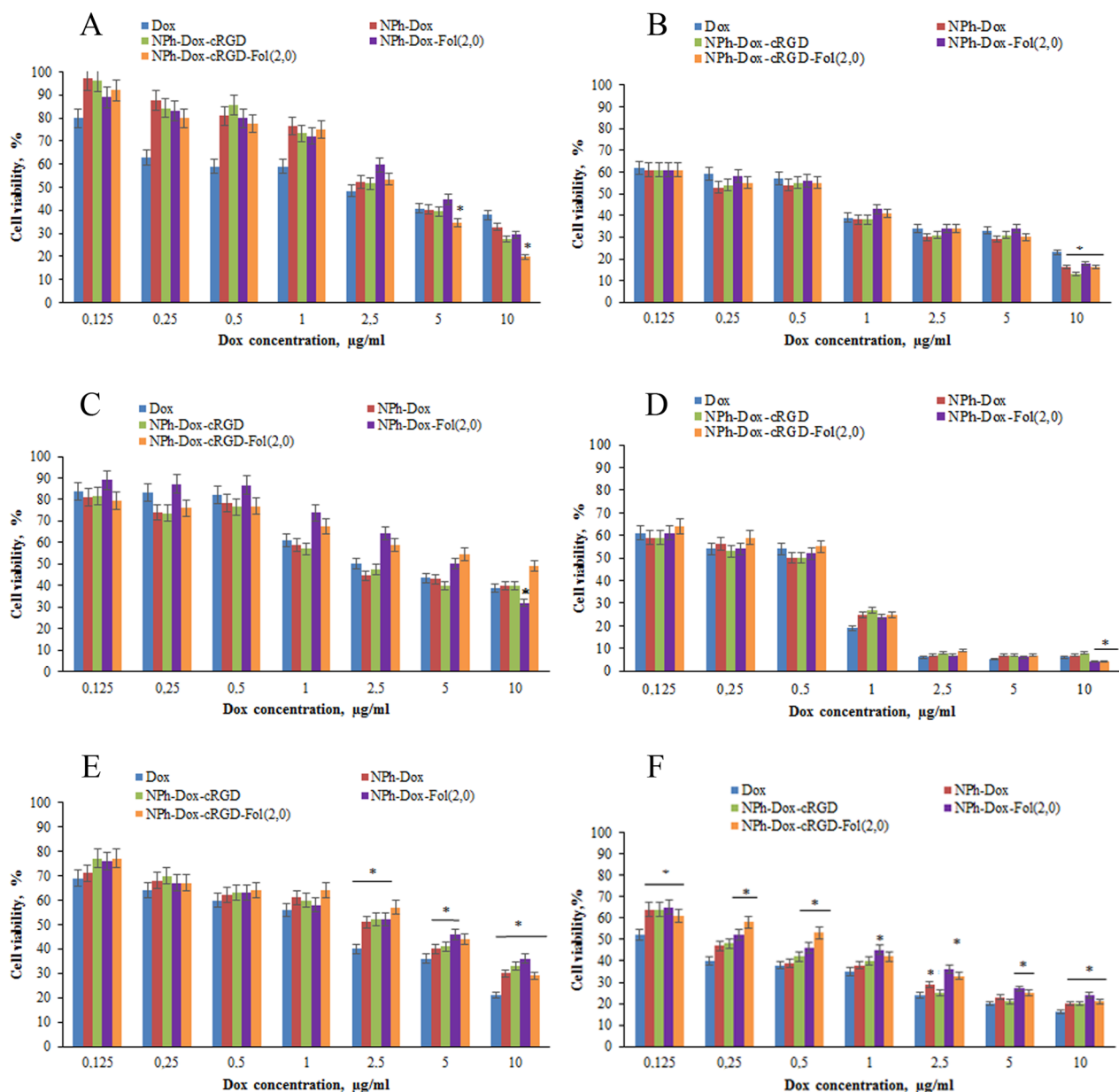


Figure 4. Viability of MDA-MB-231 (A, B), MCF-7 (C, G), and Wi-38 (D, E) cells after incubation for 24 h (A, C, D) and 48 h (B, G, E) with the Dox compositions and free Dox at different concentrations. Data are presented as mean \pm standard deviation ($n=3$). * $p < 0.05$ compared to free Dox.

Prolonged incubation with Dox compositions for 48 h decreased the percentage of living cells. In the case of MDA-MB-231 cells after 24 h at Dox up to 1 µg/ml, a more potent effect of the free substance was observed (Fig. 4A). At Dox concentrations in the samples of 2.5 µg/ml and higher, equalization of the tumor cell viability values between the compositions (about 50%) was observed. However, the percentage of living cells during incubation with NPh-Dox-Fol(2.0) was higher than for the free substance. The minimal percentage of living cells after 24 h incubation was observed for NPh-Dox-cRGD-Fol(2.0) with the Dox concentration of 10 µg/ml. After 48 h incubation, all Dox-containing constructs (in the concentration range from 0.125 µg/ml to 5 µg/ml) showed basically the same values as in the case of the free substance. This means that the Dox incorporation into NPs with vectors did not lead to a decrease in its cytostatic effect (Fig. 4B). At 10 µg/ml Dox, the maximal cell death was noted in all variants of incubation with phospholipid compositions; on average, the percentage of living cells in these samples was 30% lower than for the free substance. It should be noted that in the case of cell incubation cells with the composition containing cRGD peptide, the lowest percentage of living cells was observed as compared to the free drug (by 10%).

Among the developed compositions the most pronounced cytotoxic effect on MCF-7 cells treated with them for 24 h was found in the case of the composition containing folic acid with Dox concentrations of 5 µg/ml and 10 µg/ml (Fig. 4B). At 10 µg/ml Dox, the highest toxic effect was shown by the NPh-Dox-Fol(2.0) composition. After 48 h, the percentage of living cells treated with all studied concentrations for phospholipid samples was approximately the same as the in the case of the free substance, except 1 µg/ml Dox (Fig. 4D), where the percentage of living cells for free Dox was significantly lower than the others. In addition, starting from 2.5 µg/ml Dox, a sharp decrease in the number of living cells was observed. It should be noted that compositions containing folic acid (NPh-Dox-Fol(2.0), NPh-Dox-cRGD-Fol(2.0)) exhibited the highest toxic effect on this cell line at 10 µg/ml Dox (4% of living cells).

The study of the effect of Dox compositions on the survival of Wi-38 cells (Fig. 4D) showed that after incubation for 24 h and 48 h, the phospholipid compositions had a lesser cytotoxic effect compared to the free Dox substance, especially at Dox concentrations above 1 µg/ml. Since integrin $\alpha_v\beta_3$ is detected on the surface of Wi-38 cells [33], it was logical to assume that cRGD-containing compositions could have a negative effect due to their greater ability to bind to the receptor. However, the data obtained indicate that the monovector composition with the cRGD peptide had an effect equal to that of the phospholipid form of Dox (NPh-Dox), while the composition with two vectors had a lesser cytotoxic effect than the monovector one.

The cytotoxicity study after 48 h of incubation (Fig. 4E) showed that the compositions with Dox embedded in NPs exhibited a lower toxic effect on Wi-38 cells compared to the free substance.

In our previous studies of the tumor cell death pathway [35], it was shown that the most suitable Dox concentration for studying cell apoptosis/necrosis was 0.5 µg/ml, so this series of experiments was carried out using the this concentration of the drug. The results of the study of the mechanism of cell death of MDA-MB-231 (A), MCF-7 (B), Wi-38 (C) are shown in Figure 5.

The study on the MDA-MB-231 cell line (Fig. 5A) did not reveal any significant differences between the tested samples. However, in the case of the cRGD peptide containing composition (NPh-Dox-cRGD), there was less pronounced cell death, which followed via the apoptotic pathway (5.14% of cells subjected to early apoptosis were recorded). In the case of MCF-7 cells (Fig. 5B), a large proportion of cells subjected to necrosis was observed for all tested compositions. A lower percentage of cell death via necrosis was found in the case of NPh-Dox-Fol(2.0). On human fibroblast cells Wi-38 (Fig. 5C), cell death via apoptosis (late apoptosis) and necrosis was observed almost equally. It should be noted that a small percentage of cells subjected to early apoptosis (1–2.5%) was observed in these cells, as compared to cells of the other lines studied.

Next, we evaluated possible changes in the cell cycle of the MDA-MB-231, MCF-7, and Wi-38 cells after 24 h incubation with the studied Dox-containing compositions. The main mechanism of the antitumor effect of Dox involves DNA intercalation and DNA damage [35]. Treatment of tumors with Dox causes cell DNA damage, followed by cell senescence or temporary cell cycle arrest [36]. Therefore, it was important to evaluate the extent to which Dox incorporation into the phospholipid system containing targeting molecules could affect the change in the mechanism of drug action in tumor cells *in vitro*.

The study of the cell cycle in the MDA-MB-231 cells (Fig. 6A) showed that the NPh-Dox-cRGD-Fol(2.0) composition slightly increased the number of cells in the G0/G1 phase as compared to the control. In the case of For NPh-Dox and NPh-Dox-Fol(2.0) compositions the percentage of cells in the G0/G1 phase decreased (57–62%). In the case of Dox embedded in phospholipid NPs with/without the targeting fragments, a doubling of the peak in the G0/G1 phase, characterizing cell death by apoptosis, was observed. In the sub G0/G1 phase, the maximal increase in the percentage of cells was observed during their incubation with NPh-Dox and NPh-Dox-Fol(2.0) compositions. The phospholipid composition (NPh-Dox) with the targeting peptide (NPh-Dox-cRGD) and with folic acid (NPh-Dox-Fol(2.0)) slightly increased the percentage of cells in the S phase: this parameter

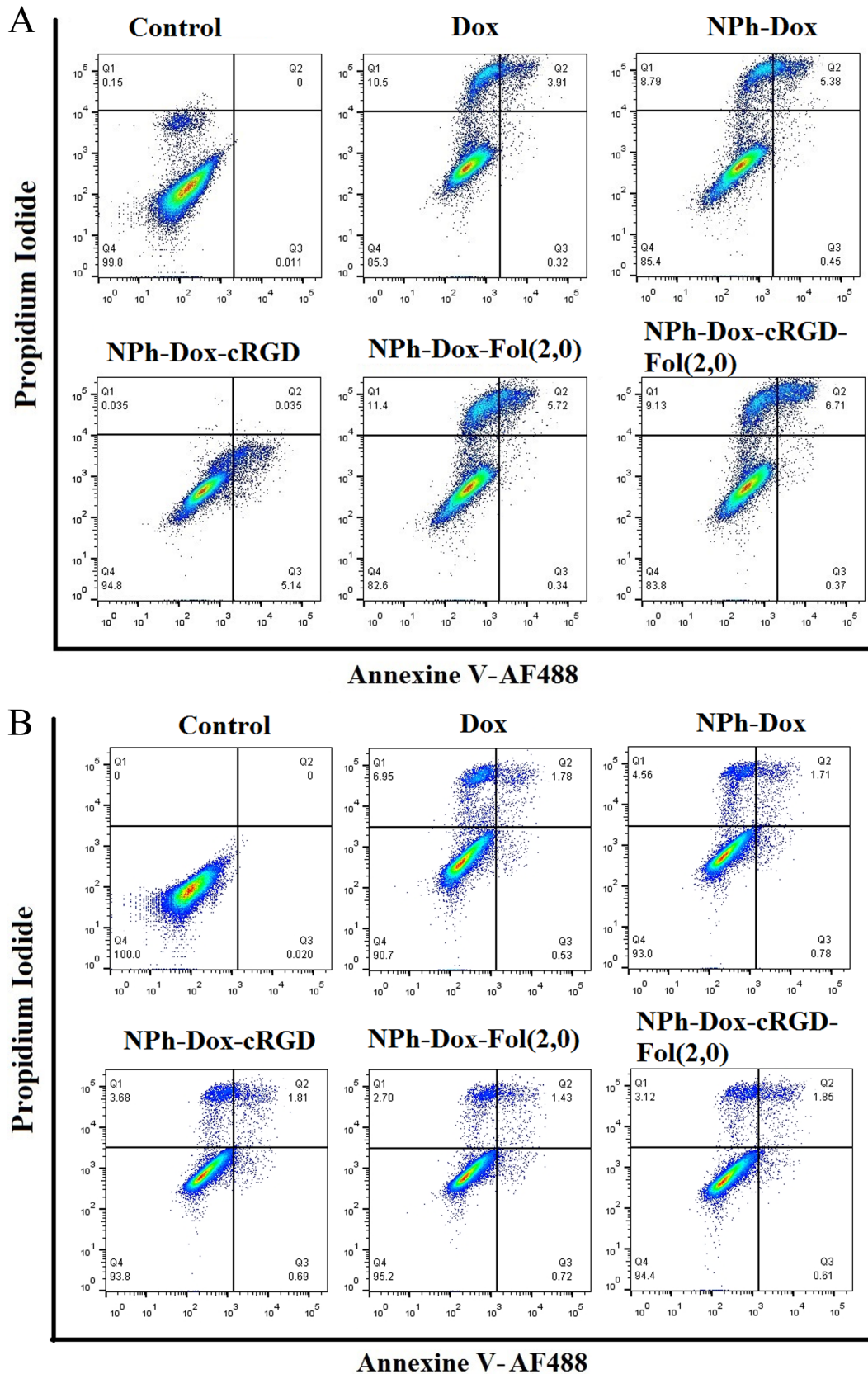


Figure 5. Analysis of apoptosis in MDA-MB-231 (A), MCF-7 (B), Wi-38 (C) cells incubated with free Dox, Dox embedded in phospholipid NPs (NPh-Dox); the phospholipid composition with a targeted peptide (NPh-Dox-cRGD); the phospholipid composition with folic acid (NPh-Dox-Fol(2,0)); the phospholipid composition with two vectors (NPh-Dox-cRGD-Fol(2,0)). Dox concentration was 0.5 $\mu\text{g/ml}$. Quadrant design: upper left (Q1): necrosis, cells stained with PI; upper right (Q2): late apoptosis; lower right (Q3): early apoptosis, cells stained with annexin V; bottom left (Q4): fluorescent signal at the level of unstained cells autofluorescence.

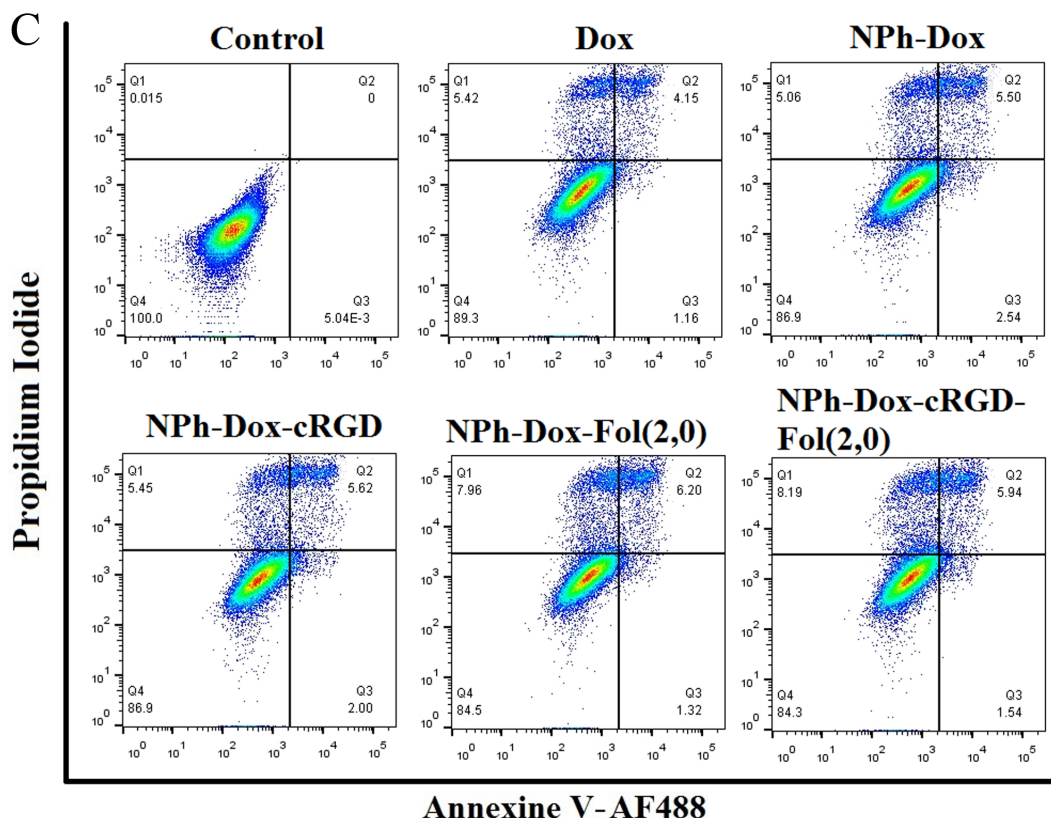


Figure 5. (continued).

did not exceed 11%. Free Dox and the NPh-Dox-Fol(2,0) composition increased the percentage of cells in the G2/M phase. However, NPh-Dox-cRGD-Fol(2,0), decreased the number of cells in this phase.

The cell cycle study using the second breast cancer cell line MCF-7 (Fig. 6B) showed no differences in the G0/G1 phase between control and Dox-treated cells. Changes (increase in the percentage of cells) were observed in the sub G0/G1 phase, with the highest values noted for the phospholipid nanoform composites and with folic acid (NPh-Dox-Fol(2,0)). In the case of the Dox composites containing folic acid (NPh-Dox-Fol(2,0) and NPh-Dox-cRGD-Fol(2,0)), cells in the S phase were not detected. It should also be noted that the phospholipid nanocomposite (NPh-Dox) decreased the percentage of cells in the G2/M phase. The study on MCF-7 cells indirectly shows that when cells are treated with NPh-Dox and NPh-Dox-Fol(2,0), they die via apoptosis.

Experiments performed on normal Wi-38 cells (Fig. 6B), revealed an increase in the percentage of cells in the G2/M phase. The highest value was shown in the case of free Dox, NPh-Dox; slightly lower values were obtained using the two-vector composition NPh-Dox-cRGD-Fol(2,0). For the same samples, a decrease in the number of cells in the G0/G1 phase was noted, and the most pronounced decrease was found in the case of NPh-Dox-cRGD-Fol(2,0). NPh-Dox-cRGD increased the percentage of cells in the G0/G1 phase. In the sub G0/G1 phase, the highest number of cells was found in the case of the two-vector

composition NPh-Dox-cRGD-Fol(2,0). This indirectly indicates cell death via apoptosis, since DNA doubling (nuclear fragmentation) occurs in this phase.

CONCLUSIONS

The effectiveness of drug action can be increased by using several targeted vectors to deliver the drugs to the tumor [18]. Using a linker of the same length for each targeting vector (DSPE-PEG2000-cRGD and DSPE-PEG2000-Folat), an increase in particle size was observed; however, the NP size for the composition studied in this work remained within 50 nm. HPLC analysis of the obtained Dox compositions with targeting conjugates showed almost complete incorporation of the drug into NPs (99%).

Dox incorporation into NPs increased both total accumulation and internalization of the cytostatic agent in the MDA-MB-231 cells expressing both FR and integrin $\alpha_v\beta_3$ (expression of FR (+), integrin $\alpha_v\beta_3$ (+)). The maximal total accumulation was noted for the two-vector composition (NPh-Dox-cRGD-Fol(2,0)). In the case of the MCF-7 breast cancer cells (FR (+), integrin $\alpha_v\beta_3$ (-)) the maximal accumulation of Dox was observed using the composition NPh-Dox-Fol(2,0); the obtained values were 2.4-fold higher than the value for the phospholipid form. In the Wi-38 cells (FR (-), integrin $\alpha_v\beta_3$ (+)) an increase in the total accumulation and internalization of Dox was observed upon incubation with the phospholipid composition (NPh-Dox).

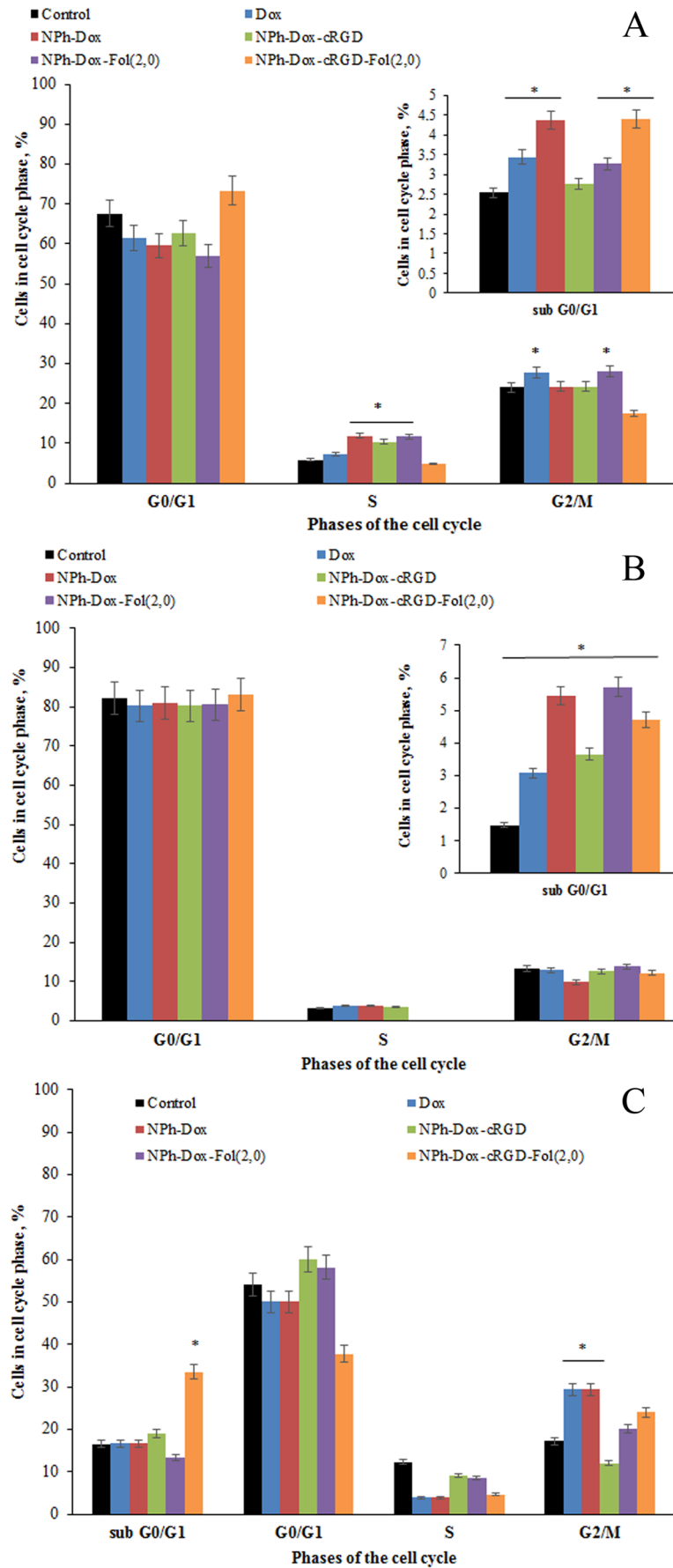


Figure 6. Graphic representation of the effect of different Dox nanoforms on the cells distribution throughout the cell cycle of MDA-MB-231 (A), MCF-7 (B), and Wi-38 (C). * $p < 0.05$ compared to control.

Although the developed compositions demonstrated dose-dependent cytotoxic effects in all studied cell lines, the Dox-containing phospholipid compositions were less toxic to control Wi-38 cells than free Dox, especially at Dox concentrations exceeding 1 µg/ml. Dox insertion into phospholipid NPs decreased drug toxicity to normal (Wi-38) cells.

The study of the cell death pathway performed using MDA-MB-231 cells showed greater contribution of the apoptotic pathway (late apoptosis), while in the case of MCF-7 cells it occurred via the necrotic pathway. This effect may be associated with the characteristics of the cells used and the duration of incubation.

Evaluation of the cell cycle change in the MDA-MB-231 cells induced by the NPh-Dox-cRGD-Fol(2.0) composition showed a slight increase in the number of cells in the G0/G1 phase compared to the control, while in the case of NPh-Dox and the NPh-Dox-Fol(2.0) composition the number of cells in the G0/G1 phase decreased. The sub G0/G1 phase peak precedes the G0/G1 phase peak, reflecting the number of apoptotic cells. In this phase, a decrease in the percentage of cells was observed in the case of NPh-Dox and NPh-Dox-Fol(2.0) compositions. In the MCF-7 cells, no differences between the samples and the control were observed in the G0/G1 phase during the cell cycle study, while an increase in the number of cells in the sub G0/G1 phase was noted for the composition NPh-Dox-Fol(2.0). In Wi-38 cells, an increase in the percentage of cells in the G2/M phase and a decrease in their number in the G0/G1 phase were shown, especially in the case of free Dox, NPh-Dox, and the two-vector composition (NPh-Dox-cRGD-Fol(2.0)). In the sub G0/G1 phase, the highest number of cells was observed during incubation with the two-vector composition (NPh-Dox-cRGD-Fol(2.0)).

Thus, the conducted *in vitro* study showed the promise of using two vectors with the same linker length for embedding into NPs for the phospholipid drug delivery system.

FUNDING

The study was supported by the Russian Science Foundation, project no. 23-25-00507, <https://rscf.ru/en/project/23-25-00507/>

COMPLIANCE WITH ETHICAL STANDARDS

This article does not contain any research involving humans or the use of animals as objects.

CONFLICT OF INTEREST

The authors declare no conflicts of interest.

REFERENCES

1. Kaprin A.D., Starinsky V.V., Shakhzadova A.O. (2024) The state of oncological care for the population of Russia in 2023; P.A. Herzen Moscow Oncology Research Institute — branch of the National Medical Research Center of Radiology of the Ministry of Health of the Russian Federation, Moscow, pp. 262.
2. Marshall S.K., Angsantikul P., Pang Z., Nasongkla N., Hussen R.S.D., Thamphiwatana S.D. (2022) Biomimetic targeted theranostic nanoparticles for breast cancer treatment. *Molecules*, **27**(19), 6473. DOI: 10.3390/molecules27196473
3. Nicoletto R.E., Ofner C.M. 3rd (2022) Cytotoxic mechanisms of doxorubicin at clinically relevant concentrations in breast cancer cells. *Cancer Chemother. Pharmacol.*, **89**(3), 285–311. DOI: 10.1007/s00280-022-04400-y
4. Sheibani M., Azizi Y., Shayan M., Nezamoleslami S., Eslami F., Farjoo M.H., Dehpour A.R. (2022) Doxorubicin-induced cardiotoxicity: an overview on pre-clinical therapeutic approaches. *Cardiovasc. Toxicol.*, **22**(4), 292–310. DOI: 10.1007/s12012-022-09721-1
5. Kong C.-Y., Guo Z., Song P., Zhang X., Yuan Y.-P., Teng T., Yan L., Tang Q.-Z. (2022) Underlying the mechanisms of doxorubicin-induced acute cardiotoxicity: oxidative stress and cell death. *Int. J. Biol. Sci.*, **18**(2), 760–770. DOI: 10.7150/ijbs.65258
6. Qin L., Wu L., Jiang S., Yang D., He H., Zhang F., Zhang P. (2018) Multifunctional micelle delivery system for overcoming resistance of doxorubicin. *J. Drug Target.*, **26**(4), 289–295. DOI: 10.1080/1061186X.2017.1379525
7. Carvalho C., Santos R.X., Cardoso S., Correia S., Oliveira P.J., Santos M.S., Moreira P.I. (2009) Doxorubicin: the good, the bad and the ugly effect. *Curr. Med. Chem.*, **16**(25), 3267–3285. DOI: 10.2174/092986709788803312
8. Ansari L., Shiehzadeh F., Taherzadeh Z., Nikoofal-Sahlabadi S., Montazi-Borojeni A.A., Sahebkar A., Eslami S. (2017) The most prevalent side effects of pegylated liposomal doxorubicin monotherapy in women with metastatic breast cancer: a systematic review of clinical trials. *Cancer Gene Ther.*, **24**(5), 189–193. DOI: 10.1038/cgt.2017.9
9. Prados J., Melguizo C., Ortiz R., Vélez C., Alvarez P.J., Arias J.L., Ruiz M.A., Gallardo V., Aranega A. (2012) Doxorubicin-loaded nanoparticles: new advances in breast cancer therapy. *Anticancer Agents Med. Chem.*, **12**(9), 1058–1070. DOI: 10.2174/187152012803529646
10. Zitzmann S., Ehemann V., Schwab M. (2002) Arginine-glycine-aspartic acid (RGD)-peptide binds to both tumor and tumor-endothelial cells *in vivo*. *Cancer Res.*, **62**(18), 5139–5143.
11. Tsai C.-C., Yang Y.-C.S.H., Chen Y.-F., Huang L.-Y., Yang Y.-N., Lee S.-Y., Wang W.-L., Lee H.-L., Whang-Peng J., Lin H.-Y., Wang K. (2023) Integrins and actions of androgen in breast cancer cells., **12**(17), 2126. DOI: 10.3390/cells12172126
12. Lan K.-C., Wei K.-T., Lin P.-W., Lin C.-C., Won P.-L., Liu Y.-F., Chen Y.-J., Cheng B.-H., Chu T.M.-G., Chen J.-F., Huang K.-E., Chang C., Kang H.-Y. (2022) Targeted activation of androgen receptor signaling in the periosteum improves bone fracture repair. *Cell Death Dis.*, **13**(2), 123. DOI: 10.1038/s41419-022-04595-1
13. Bogdanowich-Knipp S.J., Jois D.S.S., Siahaan T.J. (1999) The effect of conformation on the solution stability of linear vs. cyclic RGD peptides. *J. Pept. Res.*, **53**(5), 523–529. DOI: 10.1034/j.1399-3011.1999.00055.x
14. Bogdanowich-Knipp S.J., Chakrabarti S., Williams T.D., Dillman R.K., Siahaan T.J. (1999) Solution stability of linear vs. cyclic RGD peptides. *J. Pept. Res.*, **53**(5), 530–541. DOI: 10.1034/j.1399-3011.1999.00052.x

15. Jiang Y., Wang C., Zhang M., Liu L., Gao X., Zhang S., Ye D. (2023) Study of folate-based carbon nanotube drug delivery systems targeted to folate receptor α by molecular dynamic simulations. *Int. J. Biol. Macromol.*, **244**, 125386. DOI: 10.1016/j.ijbiomac.2023.125386
16. Zwick G.L., Mansoori G.A., Jeffery C.J. (2012) Utilizing the folate receptor for active targeting of cancer nanotherapeutics. *Nano Rev.*, **3**, 18496. DOI: 10.3402/nano.v3i0.18496
17. Mansoori G.A., Brandenburg K.S., Shakeri-Zadeh A. (2010) A comparative study of two folate-conjugated gold nanoparticles for cancer nanotechnology applications. *Cancers*, **2**(4), 1911–1928. DOI: 10.3390/cancers2041911
18. Luo W., Wen G., Yang L., Tang J., Wang J., Wang J., Zhang S., Zhang L., Ma F., Xiao L., Wang Y., Li Y. (2017) Dual-targeted and pH-sensitive doxorubicin prodrug-microbubble complex with ultrasound for tumor treatment. *Theranostics*, **7**(2), 452–465. DOI: 10.7150/thno.16677
19. Tereshkina Yu.A., Bedretidinov F.N., Kostryukova L.V. (2023) Two-vector transport phospholipid nanosystem of doxorubicin: accumulation in breast cancer cells *in vitro*. *Biomeditsinskaya Khimiya*, **69**(6), 409–419. DOI: 10.18097/PBMC20236906409
20. Song Z., Lin Y., Zhang X., Feng C., Lu Y., Gao Y., Dong C. (2017) Cyclic RGD peptide-modified liposomal drug delivery system for targeted oral apatinib administration: enhanced cellular uptake and improved therapeutic effects. *Int. J. Nanomedicine*, **12**, 1941–1958. DOI: 10.2147/IJN.S125573
21. Xu B., Yuan L., Hu Y., Xu Z., Qin J.-J., Cheng X.-D. (2021) Synthesis, characterization, cellular uptake, and *in vitro* anticancer activity of fullereneol-doxorubicin conjugates. *Front. Pharmacol.*, **11**, 598155. DOI: 10.3389/fphar.2020.598155
22. Sheldon K., Liu D., Ferguson J., Garipey J. (1995) Lologomers: design of *de novo* peptide-based intracellular vehicles. *Proc. Natl. Acad. Sci. USA*, **92**(6), 2056–2060. DOI: 10.1073/pnas.92.6.2056
23. Wan D., Liu Y., Guo X., Zhang J., Pan J. (2022) Intelligent drug delivery by peptide-based dual-function micelles. *Int. J. Mol. Sci.*, **23**(17), 9698. DOI: 10.3390/ijms23179698
24. Dinakar Y.H., Karole A., Parvez S., Jain V., Mudavath S.L. (2023) Folate receptor targeted NIR cleavable liposomal delivery system augment penetration and therapeutic efficacy in breast cancer. *Biochim. Biophys. Acta Gen. Subj.*, **1867**(9), 130396. DOI: 10.1016/j.bbagen.2023.130396
25. Tikhonova E.G., Sanzhakov M.A., Tereshkina Yu.A., Kostryukova L.V., Khudoklinova Yu.Yu., Orlova N.A., Bobrova D.V., Ipatova O.M. (2022) Drug transport system based on phospholipid nanoparticles: production technology and characteristics. *Pharmaceutics*, **14**(11), 2522. DOI: 10.3390/pharmaceutics14112522
26. Danaei M., Dehghankhold M., Ataei S., Hasanzadeh Davarani F., Javanmard R., Dokhani A., Khorasani S., Mozafari M.R. (2018) Impact of particle size and polydispersity index on the clinical applications of lipidic nanocarrier systems. *Pharmaceutics*, **10**(2), 57. DOI: 10.3390/pharmaceutics10020057
27. Bhattacharjee S. (2016) DLS and zeta potential — What they are and what they are not? *J. Control. Release*, **235**, 337–351. DOI: 10.1016/j.jconrel.2016.06.017
28. Meng F., Zhong Y., Cheng R., Deng C., Zhong Z. (2014) pH-sensitive polymeric nanoparticles for tumor-targeting doxorubicin delivery: concept and recent advances. *Nanomedicine*, **9**(3), 487–499. DOI: 10.2217/nnm.13.212
29. Gai Y., Jiang Y., Long Y., Sun L., Liu Q., Qin C., Zhang Y., Zeng D., Lan X. (2020) Evaluation of an integrin $\alpha_v\beta_3$ and aminopeptidase N dual-receptor targeting tracer for breast cancer imaging. *Mol. Pharm.*, **17**(1), 349–358. DOI: 10.1021/acs.molpharmaceut.9b01134
30. Das D., Koirala N., Li X., Khan N., Dong F., Zhang W., Mulay P., Shrikhande G., Puskas J., Drazba J., McLennan G. (2020) Screening of polymer-based drug delivery vehicles targeting folate receptors in triple-negative breast cancer. *J. Vasc. Interv. Radiol.*, **31**(11), 1866–1873.e2. DOI: 10.1016/j.jvir.2020.05.010
31. Godugu K., Sudha T., Davis P.J., Mousa S.A. (2021) Nano diamino propane tetrac and integrin $\alpha_v\beta_3$ expression in different cancer types: anti-cancer efficacy and safety. *Cancer Treat. Res. Commun.*, **28**, 100395. DOI: 10.1016/j.ctarc.2021.100395
32. Zagami R., Rapozzi V., Piperno A., Scala A., Triolo C., Trapani M., Xodo L.E., Monsù Scolaro L., Mazzaglia A. (2019) Folate-decorated amphiphilic cyclodextrins as cell-targeted nanophototherapeutics. *Biomacromolecules*, **20**(7), 2530–2544. DOI: 10.1021/acs.biomac.9b00306
33. Yoshida T., Oide N., Sakamoto T., Yotsumoto S., Negishi Y., Tsuchiya S., Aramaki Y. (2006) Induction of cancer cell-specific apoptosis by folate-labeled cationic liposomes. *J. Control. Release*, **111**(3), 325–332. DOI: 10.1016/j.jconrel.2005.12.016
34. Lanza P., Felding-Habermann B., Ruggeri Z.M., Zanetti M., Billetta R. (1997) Selective interaction of a conformationally constrained Arg-Gly-Asp (RGD) motif with the integrin receptor $\alpha_v\beta_3$ expressed on human tumor cells. *Blood Cells Mol. Dis.*, **23**(2), 230–241. DOI: 10.1006/bcmd.1997.0140
35. Kostryukova L.V., Tereshkina Y.A., Tikhonova E.G., Khudoklinova Y.Y., Bobrova D.V., Gisina A.M., Morozovich G.E., Pronina V.V., Bulko T.V., Shumyantseva V.V. (2023) Effect of an NGR peptide on the efficacy of the doxorubicin phospholipid delivery system. *Nanomaterials*, **13**(4), 2229. DOI: 10.3390/nano13152229
36. Rivankar S. (2014) An overview of doxorubicin formulations in cancer therapy. *J. Cancer Res. Ther.*, **10**(4), 853–858. DOI: 10.4103/0973-1482.139267
37. Feng X., Wu C., Yang W., Wu J., Wang P. (2022) Mechanism-based sonodynamic-chemo combinations against triple-negative breast cancer. *Int. J. Mol. Sci.*, **23**(14), 7981. DOI: 10.3390/ijms23147981

Received: 20. 11. 2024.
 Revised: 10. 12. 2024.
 Accepted: 11. 12. 2024.

ВЛИЯНИЕ ПРИСОЕДИНЕНИЯ ДВУХ АДРЕСНЫХ ВЕКТОРОВ cRGD ПЕПТИДА И ФОЛИЕВОЙ КИСЛОТЫ С ОДИНАКОВОЙ ДЛИНОЙ ЛИНКЕРА НА СВОЙСТВА ФОСФОЛИПИДНОЙ КОМПОЗИЦИИ ДОКСОРУБИЦИНА: ИССЛЕДОВАНИЕ СВОЙСТВ *IN VITRO*

Л.В. Кострюкова, Ю.А. Терешкина, Ф.Н. Бедретдинов, А.М. Гусина*

Научно-исследовательский институт биомедицинской химии им. В.Н. Ореховича,
119121, Москва, ул. Погодинская, 10; *эл. почта: kostryukova87@gmail.com

Серьёзные побочные проявления химиотерапевтического препарата доксорубицина побуждают исследователей к разработке систем его направленной доставки к клеткам-мишеням. В данной работе мы продолжили исследование по влиянию использования двух векторов в фосфолипидной системе доставки доксорубицина (Dox) для таргетной терапии рака молочной железы. Была получена композиция NPh-Dox-cRGD-Fol(2,0) с одинаковой длиной линкера для обоих адресных лигандов — cRGD и фолиевой кислоты (PEG 2000). Полученная композиция NPh-Dox-cRGD-Fol(2,0) с размером частиц менее 50 нм и с 99% встроенного в наночастицы Dox в эксперименте по высвобождению лекарства при различных значениях pH (5,0 и 7,4) показала более быстрый выход и высокий уровень Dox по сравнению с фосфолипидной наноформой и композицией, содержащей только cRGD пептид. На экспрессирующих фолатный рецептор и интегрин $\alpha_v\beta_3$ клетках рака молочной железы MDA-MB-231 в эксперименте *in vitro* было показано повышение общего накопления и интернализации Dox при инкубации с двухвекторной композицией в сравнении с контрольными образцами. На линии клеток рака молочной железы MCF-7 (экспрессирующей только фолатный рецептор) аналогичный эффект наблюдался при инкубации с одновекторной композицией, содержащей фолиевую кислоту (NPh-Dox-Fol(2,0)). На нормальной клеточной линии Wi-38 значения интернализации и общего накопления лекарства для свободной субстанции и векторных композиций были сопоставимы. Через 24 ч инкубации клеток MDA-MB-231 с Dox-содержащими (в концентрации 10 мкг/мл) образцами самый низкий процент живых клеток наблюдался для исследуемой двухвекторной композиции NPh-Dox-cRGD-Fol(2,0). На клетках MCF-7 цитотоксическое действие проявлялось в равной степени для исследуемых образцов. Исследование пути клеточной гибели на клетках MDA-MB-231 показало преобладание пути апоптоза (поздний апоптоз), а на MCF-7 — пути некроза. При исследовании клеточного цикла на линии MDA-MB-231 (фолатный рецептор (+) и интегрин $\alpha_v\beta_3$ (+)) отмечено увеличение процента клеток в фазе G0/G1, что свидетельствует об апоптотической гибели клеток при инкубации с NPh-Dox-cRGD-Fol(2,0). На клетках MCF-7 (фолатный рецептор (+) и интегрин $\alpha_v\beta_3$ (-)) различий между образцами выявлено не было.

Полный текст статьи на русском языке доступен на сайте журнала (<http://pbmc.ibmc.msk.ru>).

Ключевые слова: доксорубин; фосфолипидные наночастицы; рак молочной железы; cRGD пептид; фолиевая кислота; Faα

Финансирование. Исследование выполнено за счёт гранта Российского научного фонда № 23-25-00507, <https://rscf.ru/project/23-25-00507/>

Поступила в редакцию: 20.11.2024; после доработки: 10.12.2024; принята к печати: 11.12.2024.